Rb/Cdk2/Cdk4 triple mutant mice elicit an alternative mechanism for regulation of the G_1/S transition

Weimin Li[a,1], Shuhei Kotoshiba[a,b], Cyril Berthet[a,2], Mary Beth Hilton[a], and Philipp Kaldis[a,b,3]

[a]Mouse Cancer Genetics Program, Center for Cancer Research, National Cancer Institute, Building 560/22-56, 1050 Boyles Street, Frederick, MD 21702-1201; and [b]Cell Division and Cancer Laboratory, Institute of Molecular and Cell Biology, 61 Biopolis Drive, Proteos 03-09, Singapore 138673

Edited by Charles J. Sherr, St. Jude Children's Research Hospital, Memphis, TN, and approved November 20, 2008 (received for review May 4, 2008)

The G_1/S-phase transition is a well-toned switch in the mammalian cell cycle. Cdk2, Cdk4, and the rate-limiting tumor suppressor retinoblastoma protein (Rb) have been studied in separate animal models, but interactions between the kinases and Rb in vivo have yet to be investigated. To further dissect the regulation of the G_1 to S-phase progression, we generated Cdk2$^{-/-}$Cdk4$^{-/-}$Rb$^{-/-}$ (TKO) mutant mice. TKO mice died at midgestation with major defects in the circulatory systems and displayed combined phenotypes of Rb$^{-/-}$ and Cdk2$^{-/-}$Cdk4$^{-/-}$ mutants. However, TKO mouse embryonic fibroblasts were not only resistant to senescence and became immortal but displayed enhanced S-phase entry and proliferation rates similar to wild type. These effects were more remarkable in hypoxic compared with normoxic conditions. Interestingly, depletion of the pocket proteins by HPV-E7 or p107/p130 shRNA in the absence of Cdk2/Cdk4 elicited a mechanism for the G_1/S regulation with increased levels of p27^{Kip1} binding to Cdk1/cyclin E complexes. Our work indicates that the G_1/S transition can be controlled in different ways depending on the situation, resembling a regulatory network.

cell cycle | p27 | retinoblastoma protein | Skp2

The G_1/S-phase transition is regulated by interactions of Cdk4/6–cyclin D and Cdk2/cyclin E complexes with retinoblastoma protein (Rb) and inhibitors of the Cip/Kip or Ink4a family (1). The consequences of individual and combined ablation of these cell cycle regulators in mice have been reported. Mice lacking Cdk4 and Cdk6 exhibit late embryonic lethality and display similar phenotypes as triple cyclin D knockout animals (2, 3), implying overlapping roles of these proteins in development. However, in the absence of Cdk4 and Cdk6, Cdk2 binds to cyclin D to promote G_1-phase progression (3), indicating a cell intrinsic compensation mechanism. Indeed, combined deletion of Cdk2/4/6 does not affect mouse organogenesis until midgestation, highlighting the critical role of Cdk1 in cell cycle progression during embryonic development and cell division (4). Nevertheless, double knockout (DKO) of Cdk2 and Cdk4 affects mouse lethality and in vivo proliferation. These phenotypes have been correlated with heart defects and in mouse embryonic fibroblasts (MEFs) with impaired S-phase entry, reduced Cdk1 levels, and premature entry into senescence (5).

The inhibitory effect of p27^{Kip1} (on Cdk1) could have exacerbated the S-phase entry defects in Cdk2$^{-/-}$Cdk4$^{-/-}$ MEFs. Therefore, one would expect that deletion of p27^{Kip1} in Cdk2$^{-/-}$Cdk4$^{-/-}$ mutants should restore embryonic development and cell proliferation at least to a certain extent. A similar observation was made in the cyclin D1$^{-/-}$p27$^{-/-}$ mice, where the deletion of p27^{Kip1} rescued the phenotypic defects of cyclin D1 KO animals (6). Moreover, p27^{Kip1} is able to shuttle between cyclin D–Cdk4/6 and cyclin E/Cdk2 complexes when cyclin D levels are altered (7), reflecting the functional plasticity of p27^{Kip1}. However, there was evidence indicating that Cdk2 is not the only essential cell-cycle target of p27^{Kip1} (8, 9) and p27^{Kip1} binds to Cdk1 and inhibits its activity (8). This finding was corroborated by the fact that deletion of p27^{Kip1} in the Cdk2$^{-/-}$Cdk4$^{-/-}$ background did not affect embryonic viability and cell proliferation because the expression of Cdk1 was decreased (5). In contrast, cellular defects of Cdk2$^{-/-}$Cdk4$^{-/-}$ MEFs can be restored to a certain level by reducing the expression of pocket proteins using HPV-E7, implying a potential rescue of the phenotypes by inactivating the brakes of the E2F transcriptional circuit (5).

Rb KO mice die between mid and late gestation, owing to developmental defects in the placenta, the nervous system, and in erythropoiesis (10–13) even though proliferation rates of Rb null MEFs are comparable to wild-type cells (14, 15). In contrast, p107 or p130 KO mice are viable with different degrees of abnormalities depending on strain background (16–19). These data suggest that Rb is an important factor for cell survival and proliferation, which goes beyond its role in cell-cycle regulation (20). Although Rb plays an important role, the functions of p107 and p130 cannot be underestimated because they cooperate in the transcriptional control of the G_1/S-phase transition during embryonic development (21–23).

To assess whether deletion of Rb alone (in the presence of p107 and p130) rescues the lethality of the Cdk2/Cdk4 double mutants and to investigate how other G_1/S regulators could be involved in the control of the "restriction point," we generated Cdk2$^{-/-}$Cdk4$^{-/-}$Rb$^{-/-}$ triple mutant (TKO) mice and MEFs. Although these triple mutants died during midgestation, some of the cellular phenotypes were indeed restored. Interestingly, whereas p27^{Kip1} levels remained low in the absence of Cdk2 and Cdk4, its binding to Cdk1 was increased when the other two pocket proteins, p107 and p130, were depleted from the cells, implicating alternative mechanisms in the control of the G_1/S transition. More importantly, this finding suggests that the level of p27^{Kip1} may not be an independent indicator for cell proliferation and tumor progression when the Rb pathway is mutated or inactivated.

Results

Cdk2$^{-/-}$Cdk4$^{-/-}$Rb$^{-/-}$ Embryos Die During Midgestation. The G_1/S-phase transition and the restriction point are controlled by Rb, Cdk2, and Cdk4. Rb and Cdk2/Cdk4 regulate each other through intricate feedback loops. For example, the loss of Rb enhances E2F-mediated transcription, which increases the expression of cyclins, resulting in the activation of Cdk2 and potentially Cdk4. However, loss of Cdk2 and Cdk4 leads to hypophosphorylation of Rb, resulting in repression of E2F-mediated transcription (5). To study the genetic interactions between Rb, Cdk2, and Cdk4 in vivo, we generated TKO mice. Cdk2$^{-/-}$Cdk4$^{-/-}$Rb$^{-/-}$ (TKO) embryos were observed until embryonic day (E) 12.5 [supporting informa-

Author contributions: W.L., S.K., C.B., and P.K. designed research; W.L., S.K., and M.B.H. performed research; S.K., C.B., and P.K. contributed new reagents/analytic tools W.L., S.K., and P.K. analyzed data; and W.L., S.K., and P.K. wrote the paper.

The authors declare no conflict of interest.

This article is a PNAS Direct Submission.

[1]Present address: Department of Pharmacology, University of Wisconsin, 3725 MSC, 1300 University Avenue, Madison, WI 53706.

[2]Present address: Oncodesign, 20, Rue Jean Mazen, BP27627 Dijon Cedex 21076, France.

[3]To whom correspondence should be addressed. E-mail: kaldis@imcb.a-star.edu.sg.

This article contains supporting information online at www.pnas.org/cgi/content/full/0804177106/DCSupplemental.

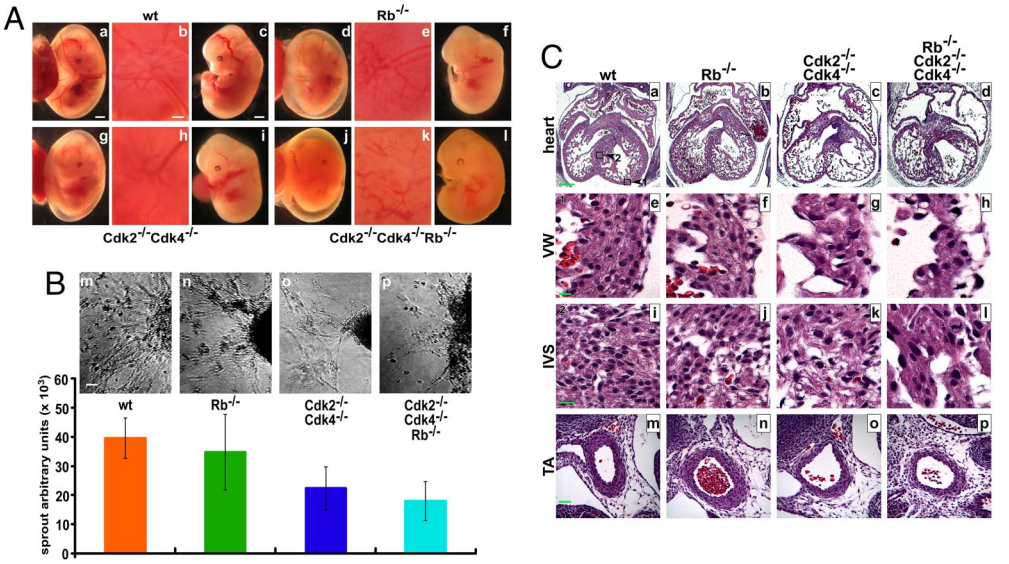

Fig. 1. TKO embryos display developmental defects in the circulatory system. (*A*) Mouse embryos at E12.5 were examined for the microvessels lining the yolk sac (*a*, *d*, *g*, *l*), placenta disk (*b*, e, *h*, *k*), and embryo body (*c*, *f*, *i*, *l*). (Scale bars: 1 mm, yolk sac and embryo; 0.5 mm, placenta disk.) (*B*) (*Upper*) Umbilical veins (*m–p*) were excised upon embryo isolation, and their angiogenic potential was evaluated by an in vitro angiogenesis assay. (Scale bar: 50 μm.) (*Lower*) The endothelial sprouts from the UV were area-quantified. (*C*) Mouse embryos were fixed and transverse sections across the heart were prepared and stained with H&E. The Cdk2$^{-/-}$Cdk4$^{-/-}$Rb$^{-/-}$, Cdk2$^{-/-}$Cdk4$^{-/-}$, and Rb$^{-/-}$ hearts displayed thin ventrical walls (VW; *e–h*) and disorganized junctions in the interventrical septum (IVS; *i–l*). In addition, the wall of the thoracic aorta (TA) (*m–p*) of TKO and DKO embryos was thin compared with wild type and Rb$^{-/-}$. (Scale bar: 200 μm, *a–d*; 10 μm, *e–l*; 40 μm, *m–p*.)

tion (SI) Table S1], indicating that TKOs die slightly earlier than Rb$^{-/-}$ (10–12) or Cdk2$^{-/-}$Cdk4$^{-/-}$ mutants (5). At E10.5, only 5% of the embryos were TKO rather than the expected 12.5% (the Cdk2 and Cdk4 loci are linked), suggesting that some of the embryos die during early embryogenesis. Analysis of the embryos indicated that the blood vessels were not as developed in the mutants (Fig. 1*A d–l*) compared with wild type (Fig. 1*A a–c*). This phenotype was observed in Rb$^{-/-}$ (Fig. 1*A d–f*), was more pronounced in Cdk2$^{-/-}$Cdk4$^{-/-}$ (Fig. 1*A g–i*) and was most prominent in TKO embryos (Fig. 1*A j–l*). To evaluate the angiogenic potential, we excised the umbilical vein from embryos and performed in vitro angiogenesis assays (Fig. 1*B* and ref. 24). The loss of Rb did not affect endothelial cell sprouting, but in the absence of Cdk2 and Cdk4, there was a 2-fold decrease in sprouting (Fig. 1*Bo*). The results for the TKO mice (Fig. 1*Bp*) were comparable with Cdk2$^{-/-}$Cdk4$^{-/-}$ mice, indicating that Rb might not contribute substantially to this phenotype, which has not previously been reported for Cdk2$^{-/-}$Cdk4$^{-/-}$ mutants.

We have described that the loss of Cdk2 and Cdk4 leads to embryonic lethality at ≈E15 because of heart defects (5). Therefore, we analyzed the morphology of the heart in wild-type, Rb$^{-/-}$, Cdk2$^{-/-}$Cdk4$^{-/-}$, and Cdk2$^{-/-}$Cdk4$^{-/-}$Rb$^{-/-}$ embryos at E12.5 (Fig. 1*C*). The hearts of Rb$^{-/-}$ embryos were comparable with wild-type heart in general, although the ventricular wall (VW) of Rb$^{-/-}$ hearts appeared to be thinner (Fig. 1*C a*, *b*, *e*, and *f*). In contrast, the heart of TKO embryos displayed a similar phenotype as the Cdk2$^{-/-}$Cdk4$^{-/-}$ heart with enlarged atria, thin VWs, and hypertrophy of the valves (Fig. 1*C c*, *d*, *g*, and *h*). In addition, the tissues of the interventricular septum (IVS) in the Rb$^{-/-}$, DKO, and TKO hearts were disorganized, and cells in the DKO and TKO IVS were larger compared with wild-type or Rb$^{-/-}$ (Fig. 1*C i–l*). The thoracic aorta (TA) of the DKO and TKO embryos was thinner than in wild type (Fig. 1*C m–p*), and there was indication of the previously described blood phenotype in Rb$^{-/-}$ embryos (10–12). These results indicate that the heart phenotype in Cdk2$^{-/-}$Cdk4$^{-/-}$ embryos is unaffected by the loss of Rb.

The loss of Rb induces increased proliferation in vivo through activation of E2F-mediated transcription at least in some tissues (for review see ref. 22). To analyze proliferation, we stained brain sections from E12.5 embryos after pulse labeling with BrdU, which is incorporated into DNA during S phase. As expected, proliferation in certain parts of the brain [striatum (ST), medulla oblongata (MO)] was increased in the absence of Rb compared with wild type (Fig. 2). Interestingly, proliferation was also increased in the brain of the TKOs (Fig. 2 *D*, *H*, *L*, *P*, and *T*) but not in Cdk2$^{-/-}$Cdk4$^{-/-}$ embryos, which indicates that the loss of Rb induces proliferation independent of Cdk2 and Cdk4.

Apoptosis in certain areas of the brain is a hallmark of Rb deficiency (10–12). Therefore, we analyzed apoptotic cells by using TUNEL assays (Fig. S1*A*). As has been reported, certain areas of Rb$^{-/-}$ brain [corpus striatum mediale (CSM), ST, MO] exhibited increased numbers of apoptotic cells (Fig. S1*A b*, *f*, *j*, and *n*). S1A In the TKO mice, the location and degree of apoptosis was similar to that in Rb$^{-/-}$ brain (Fig. S1*A d*, *h*, *l*, and *p*), whereas Cdk2$^{-/-}$Cdk4$^{-/-}$

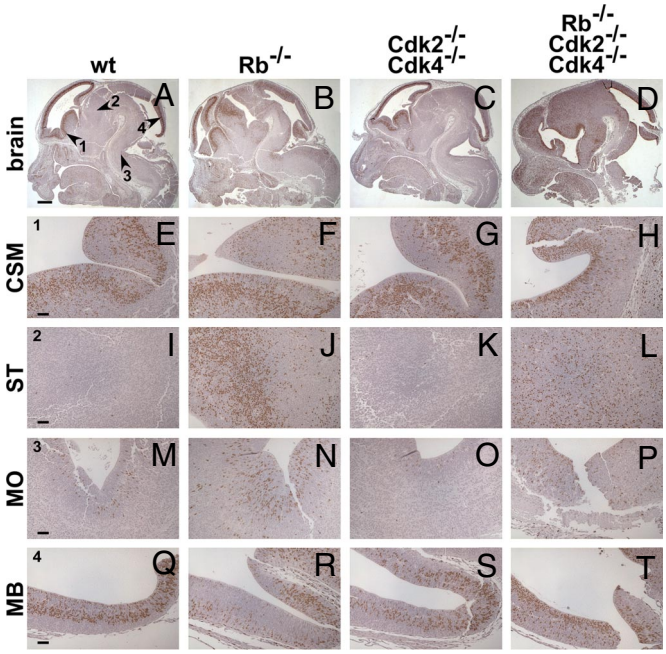

Fig. 2. Loss of Rb is associated with increased proliferation in the CNS. E12.5 mouse embryos were fixed, cryosectioned, and stained for proliferation (BrdU). Loss of Rb enhanced cell proliferation in certain compartments of the CNS (*A–D*). In ST (*I–L*) and MO (*M–P*), but not CSM (*E–H*), and midbrain (MB; *Q–T*) of the Rb$^{-/-}$ and TKO CNS cell proliferation was increased. (Scale bar: 500 μm, *A–H*; 50 μm, *E–T*).

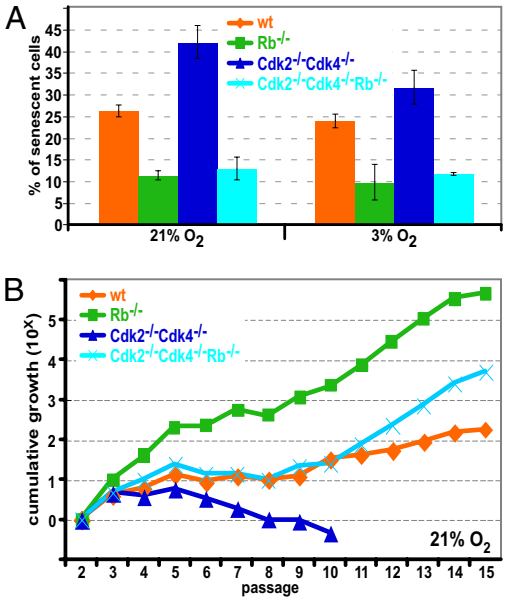

Fig. 3. Loss of Rb in MEFs decreases senescence, enhances cell proliferation, and increases cell survival. (*A*) MEFs grown at 3% or 21% oxygen were stained for β-galactosidase. At least 500 cells from 5 different fields of view were counted, and the percentage of senescent cells was plotted. (*B*) MEFs were grown at 21% O_2 and were assessed by the 3T3 assay to investigate spontaneous immortalization. Cumulative growth was plotted for each MEF line.

mutants displayed an equal number of apoptotic cells as wild type (Fig. S1*B*). Similar results were obtained for placenta (see Fig. S1*C*–*F*). Our data therefore suggest that the level of apoptosis in $Rb^{-/-}$ mouse tissues is not influenced by the loss of Cdk2 and Cdk4.

Loss of Rb Decreases Senescence and Enhances Immortalization in $Cdk2^{-/-}Cdk4^{-/-}$ MEFs. Because TKO mutants were not viable, we generated MEFs lacking Rb, Cdk2, and Cdk4. $Cdk2^{-/-}Cdk4^{-/-}$ MEFs have been reported to display severe growth defects (5); therefore, we compared growth of MEFs under normoxic conditions (21% O_2) to growth at low oxygen (3% O_2). MEFs of all genotypes grew better at 3% O_2 compared with 21% O_2 (Fig. S2). When cells are grown at 21% O_2 it is thought that a stress response is induced, which can result in senescence (25). We stained passage 2 MEFs for β-galactosidase, a marker of senescence (Fig. S3*A* and ref. 26) and found that at 3% O_2 there was a reduction of senescent cells compared with cells grown at 21% O_2, although the difference was only in the range of 10% to 20%. The lowest levels of senescence were observed in $Rb^{-/-}$ MEFs, with an ≈2-fold decrease compared with wild type (Fig. 3*A*). As reported, $Cdk2^{-/-}Cdk4^{-/-}$ MEFs enter senescence prematurely and therefore displayed increased levels of senescent cells compared with all other genotypes. Interestingly, TKO MEFs displayed the same levels of senescence as $Rb^{-/-}$ MEFs, which suggests that the induction of senescence in $Cdk2^{-/-}Cdk4^{-/-}$ MEFs depends on Rb or that the loss of Rb compensates for the loss of Cdk2 and Cdk4 to rescue the senescence phenotype.

Continuous passaging of MEFs eventually leads to spontaneous immortalization. To determine how our mutant MEFs would respond, we performed a 3T3 analysis (27). Wild-type MEFs grew exponentially in early passages and slowed down during crisis, before becoming immortalized after ≈12–15 passages (Fig. 3*B*). In contrast, an increased number of $Rb^{-/-}$ MEFs were counted in each passage compared with wild type but $Rb^{-/-}$ MEFs displayed slow growth between passages 5 and 8 nevertheless. $Cdk2^{-/-}Cdk4^{-/-}$ MEFs failed to become immortalized and died at ≈passage 10. Interestingly, TKO MEFs behaved like their wild-type counterparts and became immortal, indicating that the loss of Rb improved growth of $Cdk2^{-/-}Cdk4^{-/-}$ MEFs. In these experiments cells were cultured at atmospheric oxygen levels (21% O_2). Because growing cells at physiologically relevant conditions (3% O_2) decreases the stress response, cells tend to grow better (25). Indeed, MEFs from all genotypes became immortalized at 3% O_2 although the overall tendency was similar as when grown at 21% O_2 (Fig. S3*B*).

We performed proliferation assays with the MEFs at 3% O_2 because the 3T3 assay measures only averaged growth (Fig. S3*C*). In line with our previous data from cultures at 21% O_2 (5), $Cdk2^{-/-}Cdk4^{-/-}$ MEFs proliferated at a rate that was below the one of wild-type MEFs. In contrast, $Rb^{-/-}$ and TKO MEFs displayed a proliferation rate comparable with wild type. Furthermore, we observed a similar trend of cell proliferation in MEFs conditionally deleted for Rb (Fig. S4*A*). These experiments confirm that the loss of Rb improves the overall proliferation rate of $Cdk2^{-/-}Cdk4^{-/-}$ MEFs.

Rb Deficiency-Induced S-Phase Entry Is Associated with Increased Cdk1 Activity in TKO MEFs. To understand the mechanisms behind the improved cell growth in the absence of Rb, we examined S-phase entry after arresting MEFs in the G_0/G_1 phase by serum starvation. FACS analysis indicated that wild-type MEFs entered S phase ≈15 h after release with approximately one-third of the cells in S phase after 21 h (Fig. 4*A*; for percentage of cells in G_1 and G_2 phase see Fig. S5 *D* and *E*). $Rb^{-/-}$ MEFs entered S phase

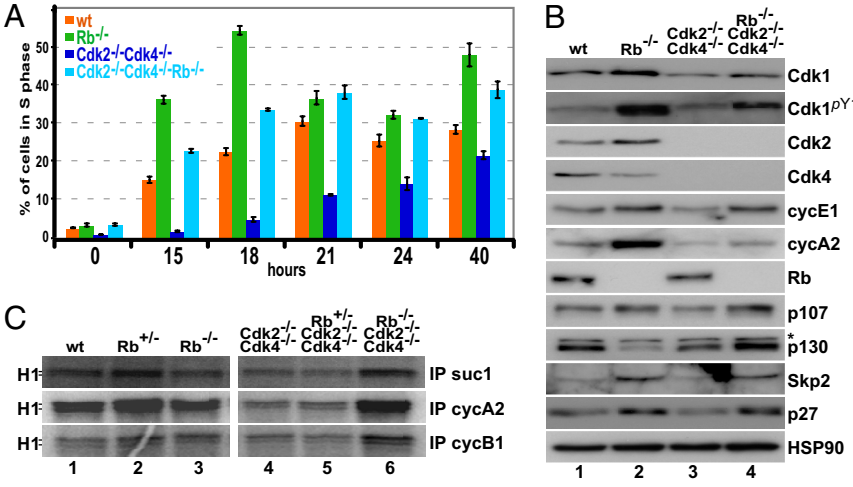

Fig. 4. Defective S-phase entry in $Cdk2^{-/-}Cdk4^{-/-}$ cells was restored by loss of Rb. (*A*) Confluent MEFs were serum-starved for 72 h at 3% O_2 and released into DMEM containing 10% FBS. Cells were BrdU-labeled, collected at the indicated time points, and analyzed by FACS. (*B*) Whole-cell extracts were prepared from unsynchronized MEFs and analyzed by Western blotting using antibodies against Cdk1, phopho-tyrosine Cdk1 ($Cdk1^{pY15}$), Cdk2, Cdk4, cyclin E1, cyclin A2, Rb, p107, p130, Skp2, $p27^{Kip1}$, and HSP90 (control). Unspecific bands are marked with ∗. (*C*) Extracts were immunoprecipitated with suc1 (binds to Cdk1 and Cdk2) and antibodies against cyclin A2 and cyclin B1. Immunoprecipitates were analyzed in vitro for associated kinase activity by using the substrate histone H1 and radiolabeled ATP.

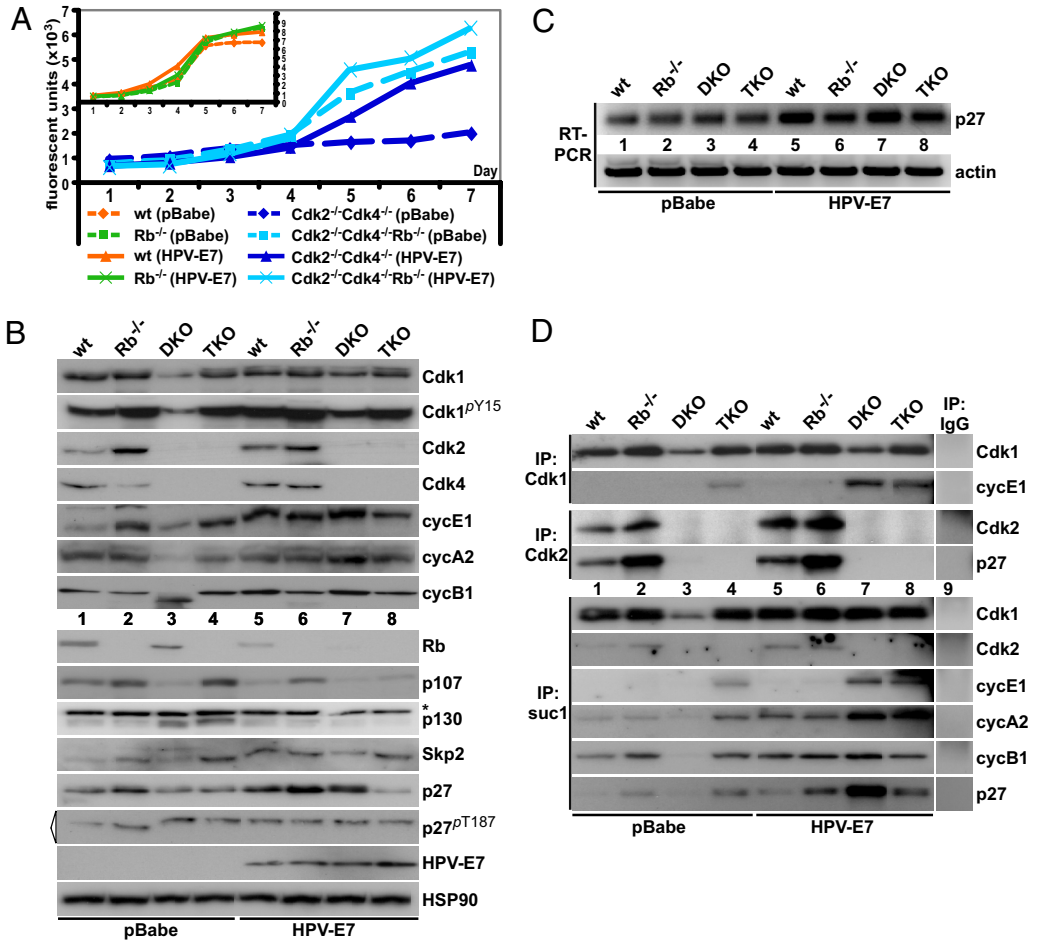

Fig. 5. Depletion of p107 and p130 in cells lacking Cdk2, Cdk4, and Rb. (*A*) Proliferation rates of MEFs infected with HPV-E7 were analyzed by using the AlamarBlue assay. (*Inset*) Control experiments with wild-type and $Rb^{-/-}$ MEFs. (*B*) Whole-cell extracts were analyzed by Western blotting using antibodies against Cdk1, phospho-tyrosine Cdk1 ($Cdk1^{pY15}$), Cdk2, Cdk4, cyclin E1, cyclin A2, Rb, p107, p130, Skp2, $p27^{Kip1}$, HPV-E7, and HSP90 (control). Levels of phospho-threonine 187 p27 ($p27^{pT187}$) were analyzed by immunoprecipitating $p27^{pT187}$ followed by blotting using antibodies against $p27^{pT187}$ (marked with a triangle). Unspecific bands are indicated by *. Control infected MEFs (pBabe) are depicted in lanes 1–4, and HPV-E7-infected cells are shown in lanes 5–8. (*C*) RT-PCR analysis of MEFs expressing HPV-E7 or vector control using primers for $p27^{Kip1}$ and β-actin. (*D*) Whole-cell extracts in *B* were immunoprecipated by using antibodies against Cdk1, Cdk2, and suc1 beads (binds to both Cdk1 and Cdk2). Immunoprecipitates were analyzed by Western blotting for changes in levels of the binding partners Cdk1, Cdk2, cyclin E1, $p27^{Kip1}$, cyclin A2, or cyclin B1. IgG controls are depicted in lane 9.

prematurely with 35% of the cells in S phase after 15 h and 55% of the cells in S phase after 18 h. Entry of $Cdk2^{-/-}Cdk4^{-/-}$ into S phase was substantially delayed. In agreement with our previous studies (5), we found only 12% of the $Cdk2^{-/-}Cdk4^{-/-}$ cells were in S phase after 24 h. Interestingly, TKO MEFs entered S phase with similar kinetics as wild-type MEFs (Fig. 4*A*), indicating that the loss of Rb promotes S-phase entry in the absence of Cdk2 and Cdk4. Similar results were obtained by conditionally deleting Rb in DKO MEFs (Fig. S4*B*).

To further investigate the molecular consequences, we analyzed the expression of various proteins (Fig. 4*B*) and Cdk kinase activity (Fig. 4*C*) in the mutant MEFs. Among the analyzed proteins, there was little difference between $Rb^{-/-}$ and wild-type MEF extracts, except that cyclin A2, cyclin E1, Skp2, and p107 were expressed at higher level because they are E2F target genes (Fig. 4*B*, compare lanes 1 and 2). In $Cdk2^{-/-}Cdk4^{-/-}$ MEF extracts, we detected decreased expression of Cdk1, cyclin A2, and cyclin E1 compared with wild type. These changes in expression were reverted to wild-type levels in the TKO MEF extracts (Fig. 4*B*, lane 4). Interestingly, the observed increase in p107 expression in $Rb^{-/-}$ and TKO MEFs (Fig. 4*B*, lanes 2 and 4) as has been described (15, 23), might account for the fact that loss of Rb cannot completely rescue some of the $Cdk2^{-/-}Cdk4^{-/-}$ phenotypes (see *Discussion*). We determined the activity of Cdk/cyclin complexes by immunoprecipitating with suc1 beads (binds to Cdk1 and Cdk2) or with antibodies against cyclin A2 (binds mostly to Cdk2 but also to Cdk1) and cyclin B1 (binds to Cdk1), followed by an in vitro kinase assay using histone H1 as substrate. The activity of Cdks was comparable in wild-type, $Rb^{+/-}$, and $Rb^{-/-}$ extracts (Fig. 4*C*, compare lanes 1–3). In the absence of Cdk2 and Cdk4, Cdk1 activity was low and was not affected by the loss of 1 copy of Rb (Fig. 4*C*, lanes 4 and 5). Nevertheless, the complete loss of Rb restored Cdk1 activity to a level comparable with that of the wild-type extract (Fig. 4*C*, lane 6). Therefore, in addition to the improved growth of TKO MEFs, we observed an increase in Cdk1 activity (see also Fig. S5 *A–C*).

The Role of p107 and p130 in the G_1/S Transition. Our results so far have indicated that the loss of Rb can compensate for the loss of Cdk2 and Cdk4 in MEFs. Nevertheless, the G_1-phase regulation is complex because p107 and p130 can compensate for the absence of Rb and we have shown that p107, but not p130, is up-regulated upon loss of Rb (Fig. 4*B*). The increased levels of p107 after deletion of Rb might have affected the results obtained from these experiments. To reduce the p107 levels, we expressed HPV-E7 (Fig. 5) or shRNAs for p107/p130 (Fig. S6) in our mutant MEFs. HPV-E7 binds to all of the pocket proteins and targets them for degradation (28). When HPV-E7 was expressed in $Cdk2^{-/-}Cdk4^{-/-}$ MEFs, the proliferation rate increased substantially, whereas only a slight increase was detected in TKO MEFs (Fig. 5*A*). Expression of HPV-E7 in wild-type or $Rb^{-/-}$ MEFs had little effect on the proliferation of these cells (Fig. 5*A Inset*). FACS analysis of the MEFs infected by HPV-E7 indicated that S-phase entry of $Cdk2^{-/-}Cdk4^{-/-}$ mutants was improved, whereas $Rb^{-/-}$ and TKO MEFs were affected only in a minor way (see Fig. S5*F*). These results indicate that the loss of Rb is the major factor in the rescue of the $Cdk2^{-/-}Cdk4^{-/-}$ phenotypes, whereas p107 and/or p130 may play a less important role.

To investigate the molecular changes in our mutant MEFs after expression of HPV-E7, we prepared cell extracts and analyzed the

expression of some of the key cell-cycle regulators (Fig. 5*B*). We found that expression of HPV-E7 did not affect the levels of Cdk1, cyclin E1, and cyclin A2 in $Rb^{-/-}$ and TKO MEFs. Interestingly, the levels of $p27^{Kip1}$ were increased in all genotypes after HPV-E7 expression with the exception of TKO MEFs. This was true for both protein and mRNA levels (Fig. 5*C*), although the increase in $p27^{Kip1}$ mRNA was most pronounced in wild-type and DKO mice. However, expression of HPV-E7 in $Cdk2^{-/-}Cdk4^{-/-}$ MEFs increased the expression of many cell-cycle regulators that we tested. These results correlate well with the observed increase in proliferation (Fig. 5*A*). In addition, we found that expression of HPV-E7 increased Tyr-15 phosphorylation of Cdk1, which did not negatively affect cell growth.

Pocket Protein Depletion Leads to an Increase of $p27^{Kip1}$/Cdk1/Cyclin E Complexes. Previously, we demonstrated Cdk1, cyclin E1, and $p27^{Kip1}$ interactions in thymus, spleen, liver, and MEF extracts (8, 29), but we did not study the complex formation of these proteins in the absence of pocket proteins. To investigate whether enhanced colocalization of Cdk1, cyclin E1, and $p27^{Kip1}$ represents a novel regulatory mechanism in cell cycle control (for immunofluorescence micrographs see Fig. S7), we performed coimmunoprecipitations using MEF extracts. First we immunoprecipitated with antibodies against Cdk1 and determined that equal amounts of Cdk1 were recovered (Fig. 5*D Top*), with the exception of $Cdk2^{-/-}Cdk4^{-/-}$ MEF extracts, in which Cdk1 was expressed at low levels (Figs. 4*B* and 5*C*). Low levels of cyclin E1 were bound to Cdk1 in wild-type extracts but increased levels coprecipitated in the absence of Rb, Cdk2, and Cdk4. The interactions of cyclin E1 with Cdk1 were further increased by the expression of HPV-E7. Binding of $p27^{Kip1}$ to Cdk1 was observed mostly after HPV-E7 expression and was more pronounced in DKO than in $Rb^{-/-}$ and TKO MEF extracts. This result was surprising because the $p27^{Kip1}$ levels in the presence of HPV-E7 were increased in wild-type, $Rb^{-/-}$, and DKO MEFs (see Fig. 5*B*, lanes 5–7) but lower in TKO MEFs. Because of this, the levels of Cdk1 bound to $p27^{Kip1}$ are not determined by the expression levels of $p27^{Kip1}$. In addition, it appears that the total level of $p27^{Kip1}$ is not correlated to the amount of Skp2 (see Fig. 5*B*, compare lanes 3 and 7). Overall, our protein analysis of cell cycle players indicated that $p27^{Kip1}$ was expressed at increased levels in the absence of the pocket proteins, but the loss of Cdk2 and Cdk4 reduced $p27^{Kip1}$ levels. This finding indicates that Rb, Cdk2, and Cdk4 regulate the levels of $p27^{Kip1}$ in a direct or indirect way. Because degradation of $p27^{Kip1}$ increases Cdk2 (and Cdk4) activity, this will feed back to Rb regulation (see *Discussion*).

Discussion

The G_1/S-phase transition is controlled by the Rb and the activity of Cdk/cyclin complexes. Here, we studied the effects of loss of Rb, Cdk2, and Cdk4 in vivo by using mouse models. The phenotypes that we observed in TKO embryos were comparable with a combination of $Rb^{-/-}$ and $Cdk2^{-/-}Cdk4^{-/-}$ mutants where embryos died ≈E13–15. In MEFs, TKOs grew as well as wild type, did not display premature entry into senescence, entered S phase without delay, and were immortalized spontaneously, which indicated that the loss of Rb rescued many $Cdk2^{-/-}Cdk4^{-/-}$ phenotypes in these cells. Expression of HPV-E7 or shRNA for p107/p130 in TKO MEFs only slightly improved growth, suggesting that unlike Rb, p107 and p130 may not play a major role in influencing the phenotypes of $Cdk2^{-/-}Cdk4^{-/-}$ mutants. Overall, our work has shown that in vivo Rb and Cdk2/Cdk4 are tightly connected in the control of the cell cycle but they also function independently from each other.

Regulation of Cdk/cyclin complexes by Rb and vice versa has been suggested to occur in a linear fashion through phosphorylation of Rb and transcription of cyclins (after derepression of E2F transcription factors), respectively. Recent results and our own data suggest that the regulation of the G_1/S transition is governed by a molecular signaling network. For example, removal of $p27^{Kip1}$ leads to a massive increase of Cdk2 and Cdk1 activity but cell-cycle progression in MEFs is unchanged (8, 30–32). One would have predicted that the increase in Cdk activity might result in hyperphosphorylation of Rb; therefore, activation of E2F-mediated transcription would be similar as in the absence of Rb. Our work was based on the assumption that if the major function of Cdk2 and Cdk4 was to phosphorylate Rb, then the phenotype of the TKO should have been similar to a $Rb^{-/-}$ mutant. However, this is not what we observed. A number of phenotypes in the TKO mutants either did not depend on Rb or Cdk2 and Cdk4. For example, the heart and the endothelial angiogenesis defects were not modified in the absence of Rb and seemed to be induced by the loss of Cdk2 and Cdk4. The endothelial angiogenesis defect is particularly interesting because it has not been described before to our knowledge and suggests that Cdk2 and Cdk4 might be regulating cell migration. Corroborating our results, it was recently described that Cdks affect cell motility and migration by phosphorylating SIRT2 (33) and $p27^{Kip1}$ has also been suggested to function in cell migration (for review see ref. 34). However, the $Rb^{-/-}$-induced apoptosis and $Rb^{-/-}$-increased proliferation was not affected by the loss of Cdk2 and Cdk4. These results do not indicate that Cdk2 and Cdk4 play no role in Rb regulation but rather that all three genes are responsible for additional functions besides the ones in the canonical Rb pathway. Some of these functions might feed back into the Rb pathway in a direct or indirect way. Therefore, future studies demonstrating downstream feedback modulations of Cdk2, Cdk4, or Rb will improve to the understanding of this regulatory network.

In our previous experiments we demonstrated that expression of HPV-E7 rescues the phenotypes of $Cdk2^{-/-}Cdk4^{-/-}$ MEFs (5). However, it was not known whether inactivation of all pocket proteins or a single pocket protein is required for the rescue of the DKO phenotypes. Our current study of $Cdk2^{-/-}Cdk4^{-/-}Rb^{-/-}$ mutants has demonstrated that the loss of Rb rescues a number of $Cdk2^{-/-}Cdk4^{-/-}$ phenotypes like growth, immortalization, senescence, and S-phase entry in MEFs. This finding indicates that p107 and p130 are not as important targets of Cdk2 and Cdk4 compared with Rb in this context. Considering that there was a substantial up-regulation of p107 when Rb was deleted, this conclusion is not as straightforward as it seems (Fig. 4*B*). Nevertheless, Rb is mostly responsible for the compensation of the $Cdk2^{-/-}Cdk4^{-/-}$ phenotypes. Maybe the rescue could have been more complete if the levels of p107 remained similar compared with wild type. Silencing of p107 using shRNA retroviruses did not significantly affect the growth of DKO and TKO MEFs. One of the possible reasons that loss of Rb is sufficient to rescue the $Cdk2^{-/-}Cdk4^{-/-}$ phenotypes might be that Rb is uniquely suited to regulate transcription of Cdk1 because increased Cdk1 levels and activity seems to be essential for the rescue. Therefore, the loss of p107 and p130 might not be able to drive the transcription of Cdk1 efficiently in vivo.

One of the remarkable observations in the TKO MEFs was the control of $p27^{Kip1}$ expression. In the absence of Rb, we observed increases in $p27^{Kip1}$, cyclin E1, and p107 levels (Fig. 4*B*). The situation was different when HPV-E7 was expressed and $p27^{Kip1}$ levels increased substantially, especially in the $Cdk2^{-/-}Cdk4^{-/-}$ MEFs, whereas p107 levels decreased (Fig. 5*B*). We believe this finding is interesting because cell cycle progression was rather improved in the absence of all pocket proteins but it was accompanied by increased levels of $p27^{Kip1}$ and increased Cdk1/cyclin E1/$p27^{Kip1}$ complex formation. This might indicate that pocket proteins regulate the ratio of Skp2 and $p27^{Kip1}$. Corroborating our results, there were other reports that suggested tight coupling between pocket proteins and $p27^{Kip1}$. For example, it was proposed that p130 displays "p27-like" abilities to inhibit Cdk2, especially in the absence of $p27^{Kip1}$ (35). Rb has also been reported to interact with Skp2 and interfere with Skp2-$p27^{Kip1}$ interactions, which inhibits ubiquitination of $p27^{Kip1}$ (36). Others have suggested that there is a Skp2 autoinduction loop, consisting of Rb (E2F), Skp2,

and $p27^{Kip1}$ (Cdk2/cycE) (37). Furthermore, in the triple knockout MEFs of Rb/p107/p130, $p27^{Kip1}$ becomes essential to arrest cells in G_2 (38, 39). Our results and these reports suggest that ablation of pocket proteins affects (*i*) the ratio of Skp2 and $p27^{Kip1}$ directly or indirectly and (*ii*) $p27^{Kip1}$ degradation are uncoupled from Skp2 levels in the pocket protein depleted cells.

Our work has highlighted the intricate regulation of the G_1/S-phase transition by Rb, Cdk2, Cdk4, and $p27^{Kip1}$. The compensatory interactions of Cdk1 and $p27^{Kip1}$ in the control of the cell-cycle progression from G_1 to S phase provide an alternative mode in special circumstances. In the context of mutation of the pocket protein pathway during tumorigenesis, $p27^{Kip1}$ might not serve as a definite factor for prognosis. Nevertheless, there is a lot more to learn on how this network is organized to efficiently control the G_1/S-phase transition.

Materials and Methods

Mouse Strains, Embryos, Cells, Histology and Immunohistochemistry. $Cdk2^{+/-}Cdk4^{+/-}Rb^{+/-}$ triple heterozygotes mice were generated by crossing $Cdk2^{+/-}Cdk4^{+/-}$ (C57BL/6 background) and $Rb^{+/-}$ mice (129S1/SvImJ background, from $Rb^{flox/flox}$ (ref. 40; kindly provided by Anton Berns, The Netherlands Cancer Institute (NKI), Amsterdam, Netherlands) mice crossed with the ß-actin-Cre strain). Triple heterozygotes were then intercrossed to generate wild-type, $Rb^{-/-}$, $Cdk2^{-/-}Cdk4^{-/-}$ (DKO), and $Cdk2^{-/-}Cdk4^{-/-}Rb^{-/-}$ (TKO) embryos and MEFs. Primary MEFs were generated as described (41). Pregnant mice were injected i.p. with BrdU 2 h before the embryos were collected and fixed before histological processing. In brief, transverse heart sections were stained with H&E. The embryo heads were sectioned sagittally, and alternative sections from head were stained with an ApopTag kit (Millipore) for apoptosis or antibodies against BrdU (Invitrogen) for proliferation according to the manufacturer's instructions.

In Vitro Angiogenesis Assay. Umbilical veins were isolated from the embryos, cut into 0.5-mm-long pieces under the microscope, and embedded in fibrin gel, which was overlaid with DMEM containing 10% FBS. Endothelial sprouts from the umbilical veins were imaged and quantified by computerized systems (24).

Analysis of MEFs. Primary MEFs were seeded in chamber slides and stained for SA-β-galactosidase as described (5). The 3T3 and proliferation assay have been described (5). HPV16-E7 or PGK-Cre was cloned into the retroviral vector pBabe, and MEFs were infected as described (5). Cells were synchronized, labeled with BrdU, and analyzed by FACS analysis as described (5). MEFs were fixed and stained as described (29). MEF total RNA was extracted by using the TRIzol reagent and analyzed as described (5).

Immunoblotting, Immunoprecipitation, and Kinase Assay. MEFs were used for Western blot analysis or kinase assays as described (42). Antibodies used in this study were: Cdk1 and Cdk2 as described (41), Phospho-Cdk1(Tyr-15) (Cell Signaling Technology 9111S), cyclin E1 (eBioscience 14-6714-63), p107 (eBioscience 14-6744-81), cyclin D1(NeoMarkers RB-010-P), cyclin A2 (Santa Cruz Biotechnology SC-751), cyclin B1 (Santa Cruz SC-245), HPV16-E7 (Santa Cruz SC-6981), Skp2 (Santa Cruz SC-7164), Rb (BD Biosciences 554136), p130 (BD Biosciences 610262), $p27^{Kip1}$ (BD Biosciences 610242), HSP90 (BD Biosciences 610418), and phospho-$p27^{T187}$ (Invitrogen 37-9700). For immunoprecipitation and kinase assays, cross-linked antibodies against Cdk2 and cyclin B1 [as described (41)], anti Cdk1 (Santa Cruz SC-54 AC), anti-cyclin A2 (Santa Cruz SC-751 AC), and suc1 agarose beads (Millipore 14-132) were used.

Additional Methods. Full-length descriptions of materials and methods can be found in *SI Text*.

ACKNOWLEDGMENTS. We thank Matt McCollum and Angie Smith for animal care; Anton Berns for the $Rb^{flox/flox}$ mice; Keith Rogers, Donna Butcher, Roberta Smith, and the Pathology/Histotechnology Laboratory, National Cancer Institute for tissue sectioning and staining; Jerrold Ward for the placenta pathology; Stephen J. Lockett for helping with confocal microscopy; Julien Sage (Stanford University, Stanford, CA) for shRNA vectors for p107/p130; members of P.K.'s laboratory for discussions and support; and Stefan Lim, Shuhui Lim, and Kasim Diril for comments on the manuscript. This work was supported by the Intramural Research Program of the National Institutes of Health, National Cancer Institute, Center for Cancer Research, and A*STAR of Singapore.

1. Morgan DO (1997) Cyclin-dependent kinases: Engines, clocks, and microprocessors. *Annu Rev Cell Dev Biol* 13:261–291.
2. Kozar K, *et al.* (2004) Mouse development and cell proliferation in the absence of D-cyclins. *Cell* 118:477–491.
3. Malumbres M, *et al.* (2004) Mammalian cells cycle without the D-type cyclin-dependent kinases Cdk4 and Cdk6. *Cell* 118:493–504.
4. Santamaria D, *et al.* (2007) Cdk1 is sufficient to drive the mammalian cell cycle. *Nature* 448:811–815.
5. Berthet C, *et al.* (2006) Combined loss of Cdk2 and Cdk4 results in embryonic lethality and Rb hypophosphorylation. *Dev Cell* 10:563–573.
6. Geng Y, *et al.* (2001) Deletion of the $p27^{Kip1}$ gene restores normal development in cyclin D1-deficient mice. *Proc Natl Acad Sci USA* 98:194–199.
7. Sherr CJ, Roberts JM (1999) Cdk inhibitors: Positive and negative regulators of G_1-phase progression. *Genes Dev* 13:1501–1512.
8. Aleem E, Kiyokawa H, Kaldis P (2005) Cdc2–cyclin E complexes regulate the G_1/S-phase transition. *Nat Cell Biol* 7:831–836.
9. Martin A, *et al.* (2005) Cdk2 is dispensable for cell cycle inhibition and tumor suppression mediated by $p27^{Kip1}$ and $p21^{Cip1}$. *Cancer Cell* 7:591–598.
10. Clarke AR, *et al.* (1992) Requirement for a functional Rb-1 gene in murine development. *Nature* 359:328–330.
11. Jacks T, *et al.* (1992) Effects of an Rb mutation in the mouse. *Nature* 359:295–300.
12. Lee EY, *et al.* (1992) Mice deficient for Rb are nonviable and show defects in neurogenesis and hematopoiesis. *Nature* 359:288–294.
13. Wu L, *et al.* (2003) Extra-embryonic function of Rb is essential for embryonic development and viability. *Nature* 421:942–947.
14. Herrera RE, *et al.* (1996) Altered cell cycle kinetics, gene expression, and G_1 restriction point regulation in Rb-deficient fibroblasts. *Mol Cell Biol* 16:2402–2407.
15. Sage J, Miller AL, Perez-Mancera PA, Wysocki JM, Jacks T (2003) Acute mutation of retinoblastoma gene function is sufficient for cell cycle re-entry. *Nature* 424:223–228.
16. Cobrinik D, *et al.* (1996) Shared role of the pRB-related p130 and p107 proteins in limb development. *Genes Dev* 10:1633–1644.
17. LeCouter JE, *et al.* (1998) Strain-dependent myeloid hyperplasia, growth deficiency, and accelerated cell cycle in mice lacking the Rb-related p107 gene. *Mol Cell Biol* 18:7455–7465.
18. LeCouter JE, Kablar B, Whyte PF, Ying C, Rudnicki MA (1998) Strain-dependent embryonic lethality in mice lacking the retinoblastoma-related p130 gene. *Development* 125:4669–4679.
19. Lee MH, *et al.* (1996) Targeted disruption of p107: Functional overlap between p107 and Rb. *Genes Dev* 10:1621–1632.
20. Yamasaki L (2006) Modeling cell cycle control and cancer with pRB tumor suppressor. *Cell Cycle Regulation: Results and Problems in Cell Differentiation*, ed Kaldis P (Springer, Heidelberg), Vol 42, pp 227–256.
21. Dannenberg J-H, van Rossum A, Schuijff L, te Riele H (2000) Ablation of the retinoblastoma gene family deregulates G_1 control, causing immortalization and increased cell turnover under growth-restricting conditions. *Genes Dev* 14:3051–3064.
22. Dannenberg JH, te Riele HP (2006) The retinoblastoma gene family in cell cycle regulation and suppression of tumorigenesis. *Cell Cycle Regulation: Results and Problems in Cell Differentiation*, ed Kaldis P (Springer, Heidelberg), Vol 42, pp 183–225.
23. Sage J, *et al.* (2000) Targeted disruption of the three Rb-related genes leads to loss of G_1 control and immortalization. *Genes Dev* 14:3037–3050.
24. Li W, *et al.* (2007) Hypoxia-induced endothelial proliferation requires both mTORC1 and mTORC2. *Circ Res* 100:79–87.
25. Parrinello S, *et al.* (2003) Oxygen sensitivity severely limits the replicative lifespan of murine fibroblasts. *Nat Cell Biol* 5:741–747.
26. Dimri GP, *et al.* (1995) A biomarker that identifies senescent human cells in culture and in aging skin in vivo. *Proc Natl Acad Sci USA* 92:9363–9367.
27. Todaro GJ, Green H (1963) Quantitative studies of the growth of mouse embryo cells in culture and their development into established lines. *J Cell Biol* 17:299–313.
28. Münger K, Howley PM (2002) Human papillomavirus immortalization and transformation functions. *Virus Res* 89:213–228.
29. Satyanarayana A, Hilton MB, Kaldis P (2008) p21 inhibits Cdk1 in the absence of Cdk2 to maintain the G_1/S-phase DNA damage checkpoint. *Mol Biol Cell* 19:65–77.
30. Fero ML, *et al.* (1996) A syndrome of multiorgan hyperplasia with features of gigantism, tumorigenesis, and female sterility in $p27^{Kip1}$-deficient mice. *Cell* 85:733–744.
31. Kiyokawa H, *et al.* (1996) Enhanced growth of mice lacking the cyclin-dependent kinase inhibitor function of $p27^{Kip1}$. *Cell* 85:721–732.
32. Nakayama K, *et al.* (1996) Mice lacking $p27^{Kip1}$ display increased body size, multiple organ hyperplasia, retinal dysplasia, and pituitary tumors. *Cell* 85:707–720.
33. Pandithage R, *et al.* (2008) The regulation of SIRT2 function by cyclin-dependent kinases affects cell motility. *J Cell Biol* 180:915–929.
34. Besson A, Dowdy SF, Roberts JM (2008) CDK inhibitors: Cell cycle regulators and beyond. *Dev Cell* 14:159–169.
35. Coats S, *et al.* (1999) A new pathway for mitogen-dependent Cdk2 regulation uncovered in $p27^{Kip1}$-deficient cells. *Curr Biol* 9:163–173.
36. Ji P, *et al.* (2004) An Rb–Skp2–p27 pathway mediates acute cell cycle inhibition by Rb and is retained in a partial-penetrance Rb mutant. *Mol Cell* 16:47–58.
37. Yung Y, Walker JL, Roberts JM, Assoian RK (2007) A Skp2 autoinduction loop and restriction point control. *J Cell Biol* 178:741–747.
38. Foijer F, Wolthuis RM, Doodeman V, Medema RH, Te Riele H (2005) Mitogen requirement for cell cycle progression in the absence of pocket protein activity. *Cancer Cell* 8:455–466.
39. Foijer F, Te Riele H (2006) Restriction beyond the restriction point: Mitogen requirement for G_2 passage. *Cell Div* 1:8.
40. Marino S, Vooijs M, van Der Gulden H, Jonkers J, Berns A (2000) Induction of medulloblastomas in p53-null mutant mice by somatic inactivation of Rb in the external granular layer cells of the cerebellum. *Genes Dev* 14:994–1004.
41. Berthet C, Aleem E, Coppola V, Tessarollo L, Kaldis P (2003) Cdk2 knockout mice are viable. *Curr Biol* 13:1775–1785.
42. Satyanarayana A, *et al.* (2008) Genetic substitution of Cdk1 by Cdk2 leads to embryonic lethality and loss of meiotic function of Cdk2. *Development* 135:3389–3400.